

## Quantification of Total Mercury in Antarctic Surface Snow using ICP-SF-MS: Spatial Variation from the Coast to Dome Fuji

Yeongcheol Han, Youngsook Huh,\* Sungmin Hong,<sup>†</sup> Soon Do Hur,<sup>‡</sup> Hideaki Motoyama,<sup>§</sup> Shuji Fujita,<sup>§</sup> Fumio Nakazawa,<sup>§</sup> and Kotaro Fukui<sup>§</sup>

*School of Earth and Environmental Sciences/RIO, Seoul National University, Seoul 151-747, Korea. \*E-mail: yuhuh@snu.ac.kr*

*<sup>†</sup>Department of Ocean Sciences, Inha University, Incheon 402-751, Korea*

*<sup>‡</sup>Korea Polar Research Institute, Songdo Techno Park, Incheon 406-840, Korea*

*<sup>§</sup>National Institute of Polar Research, 10-3, Midoricho, Tachikawa, Tokyo 190-8518, Japan*

*Received July 2, 2011, Accepted October 9, 2011*

The total mercury concentration ( $Hg_T$ ) of surface snow samples collected along a ~1500 km transect in east Queen Maud Land was determined using inductively coupled plasma sector field mass spectrometry to address the behavior of Hg on the Antarctic Plateau. Due to the volatile nature of mercury, measures were taken against Hg loss from standard solutions by choosing appropriate container material and stabilizing agents. Glass bottles with Teflon-lined caps were superior to Teflon and polyethylene containers in protecting against Hg loss, but addition of gold chloride ( $AuCl_3$ ) or bromine chloride ( $BrCl$ ) was necessary to ensure preservation of Hg. As Hg loss was also observed in snowmelt samples, our analysis may underestimate the actual amount of  $Hg_T$  in the snow. Even so, the measured  $Hg_T$  was still very low ( $< 0.4$ – $10.8$   $pg\ g^{-1}$ ,  $n = 44$ ) without a signal of depositional enhancement accompanying photo-oxidation of atmospheric elemental mercury in austral mid-summer. Moreover, the dynamic variation along the traverse implies spatial and temporal heterogeneity in its source processes.

**Key Words :** Gaseous elemental mercury, Reactive gaseous mercury, Atmospheric mercury depletion event, Photochemical oxidation and reduction

### Introduction

The thick snowpack covering the vast Antarctic continent acts as a perennial sink for various trace metals.<sup>1</sup> Because gaseous elemental mercury (GEM,  $Hg^0$ ) has a long atmospheric residence time of 6–24 months,<sup>2</sup> it can be transported from distant sources and deposit onto the Antarctic snowpack.<sup>3</sup>

The sequestration of atmospheric Hg by polar snowpack results from an imbalance between the dry/wet deposition and re-emission principally governed by photochemical redox chemistry.<sup>4,5</sup> For example, the atmospheric mercury depletion event (AMDE) is the rapid disappearance of atmospheric GEM in spring as a result of its photo-oxidation to reactive gaseous mercury (RGM,  $Hg^{II}$ ) and subsequent deposition onto surface snow.<sup>6,7</sup> The phenomenon of AMDE has been documented through atmospheric measurements, first at Alert in the Arctic<sup>8</sup> then in several Arctic<sup>4,5</sup> and a few Antarctic sites,<sup>9</sup> which tends to occur with abundant marine halogen supply from nearby sea-ice. The deposition instantly elevates Hg levels in the surface snow, although it can be re-emitted as GEM through photochemical reduction.<sup>10</sup>

Recent studies of snow samples from Antarctica reported elevated total mercury ( $Hg_T$ ) concentrations which were attributed to enhanced atmospheric GEM oxidation. This has been observed both in the inland sites far from direct marine halogen supply, at South Pole ( $198$   $pg\ g^{-1}$ )<sup>11</sup> and Concordia (several hundred  $pg\ g^{-1}$ )<sup>12</sup> as well as in the sea-ice region

near McMurdo ( $70$ – $430$   $pg\ g^{-1}$ )<sup>13</sup> (Table 1, Fig. 1). These observations stand in contrast to previous studies which reported low  $Hg_T$  values both for the inland and coastal snow samples ( $< 40$   $pg\ g^{-1}$ , Table 1). One possible reason may be that prior to the first documentation of AMDE in 1998, high  $Hg_T$  levels in snow had been attributed to contamination.<sup>14</sup> As the snowpack over the vast Antarctic Plateau ( $> 5$  million  $km^2$ ) may play an important role in the global Hg cycle, the wide variation of  $Hg_T$  of Antarctic snow in the literature needs to be evaluated precisely. Existing data sets are not systematic enough, temporally and spatially, to constrain important parameters such as distance from the coast, atmospheric circulation pattern, topography, and sampling season. One objective of this study was to add new  $Hg_T$  data for Antarctic surface snow with large spatial coverage within a relatively short sampling period (1.5 months).

Determination of  $Hg_T$  in the snowmelt is challenging because various Hg species (i.e. organic, inorganic and particulate) occur at very low levels ( $< 1$   $pg\ g^{-1}$ ; Table 1), while some species are even volatile (e.g.  $Hg^0$ ,  $(CH_3)_2Hg$ ). The inductively coupled plasma sector field mass spectrometry (ICP-SF-MS) offers a number of advantages over the conventional cold vapor generation method for determining  $Hg_T$  by reducing sample consumption, by eliminating complicated pretreatment steps, and by promoting decomposition of nonreactive or strongly bound mercury.<sup>15</sup> However it should be noted that the volatility of mercury, regarded as an advantage for the cold vapor generation method, can cause

**Table 1.** Published mercury concentrations in Antarctic snow

Location	Distance from coast (km)	Altitude (m)	Sampling date (yyyy/mm/dd)	Hg ( $\mu\text{g g}^{-1}$ )	Analytical method	Sample type	Reference
McMurdo	-30 ~ 0	0	2003/11/03-04	40-430 (n=24)	CVAFS	Surface snow on sea-ice	13
South victoria land	5	2200	1988/12/30-31	0.4-1.5 (n=5)	Photoacoustic Hg analyzer	Surface snow	3
Taylor valley	10	678	2004	0.3-40 (n=32)	CVAFS	Snow pit	37
Dome F traverse	<b>30-800</b>	<b>948-3809</b>	<b>2007/11/14-2008/01/19</b>	<b>&lt; 0.4-10.8 (n=44)</b>	<b>ICP-SF-MS</b>	<b>Surface snow</b>	<b>This study</b>
Dumont d'Urville traverse (Adelie Land-Dome C)	33 103 433	848 1500 2525	1983/01 1983/01 1983/01	0.50 0.20 0.13	CVAFS CVAFS CVAFS	Age 1982/09-1983/01 Age 1982/06-1983/01 Age 1982/06-1983/01	38
Halley (Coats Land)	200	1420	1986-1987/Summer	0.2-16.1 (n=170)	ICP-SF-MS	Depth 0-16.3 m Age 1834-1986	15
Concordia	1070	3240	Not reported	Hundreds	Not reported	Not reported	12
South Pole	1274	2880	1984/01	0.25	CVAFS	Age 1982/11-1984/01	38
South Pole	1274	2880	2005/11/16	198 (n=3)	Not reported	Surface snow	11

CVAFS: Cold Vapor Atomic Fluorescence Spectrometry

bias due to mercury loss from solutions prior to introduction into the ICP.<sup>16</sup> Single elemental mercury solutions prepared with dilute nitric acid is known to be extremely unstable,<sup>15,16</sup> and another objective of this study was to investigate the loss of volatile Hg in artificial standard solutions so that one can properly evaluate such loss in natural snowmelt samples.

### Experimental

Snow samples were obtained during the Japanese-Swedish Antarctic Expedition (JASE) which took place between November 2007 and January 2008 as part of the International Trans Antarctic Scientific Expedition (ITASE) program. Surface snow samples were collected at 147 locations over a distance of ~3000 km (1500 km one way) from the Syowa Station near the coast via Dome Fuji to the Turning Point (75.88°S, 25.83°E) before returning to the Syowa Station (Fig. 1). Snow samples were transferred to thoroughly pre-cleaned 1 L LDPE bottles double sealed in acid-cleaned LDPE bags and kept frozen in the dark until further processing. Details on cleaning and sample handling protocols can be found in the reference.<sup>18</sup>

Of the 147 surface snow samples collected during the expedition, 44 were subsampled and analyzed for  $\text{Hg}_T$  (Fig. 1). Thirty five samples (hereafter referred to as SS1) were thawed at room temperature in a class 10 clean bench at the Korea Polar Research Institute (KOPRI). After complete melting which took less than 6 hours, ~5 mL aliquots for  $\text{Hg}_T$  analyses were stored in pre-cleaned 15 mL LDPE bottles and kept frozen in the dark. They were thawed and acidified to 2%  $\text{HNO}_3$  just prior to ICP-SF-MS analyses. For nine samples (hereafter referred to as SS2), we skipped the second storage step by thawing, aliquoting, and acidifying the snow samples in the sample introduction area of the

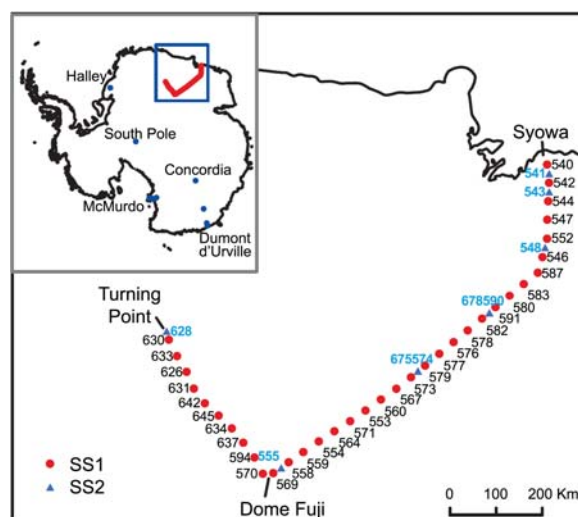


**Figure 1.** Sample location along the traverse from the Syowa station via Dome Fuji to the Turning Point and back. Site numbers are indicated for the SS1 series (analyzed after aliquoting and storage) and SS2 series (analyzed immediately after aliquoting). Samples 574 and 675 and samples 590 and 678 were collected at the same sites but at different times. Locations for which snow Hg data are available in the literature (Table 1) are shown on the inset. South Victoria Land and Taylor Valley are located close to McMurdo.

ICP-SF-MS and analyzing them immediately. It took less than 15 minutes from aliquoting to the end of analysis for each sample. The SS2 samples were refrozen until re-analysis carried out a month later.

Snow samples were analyzed on Thermo Scientific ELEMENT2 ICP-SF-MS installed at the National Center for Inter-university Research Facilities (NCIRF) at Seoul National University. The detection limit estimated as three times the standard deviation of the blank (n = 9) was 0.4  $\mu\text{g}$

$\text{g}^{-1}$  or about  $0.8 \text{ pg}$  under our experimental conditions. See Supplementary Material for details on instrumental setting, calibration, blank, and wash procedures.

We prepared  $20 \text{ pg g}^{-1}$  Hg standard solutions to assess the temporal loss of Hg as a function of container material and preservative. The solutions were rapidly diluted from freshly prepared  $100 \text{ ng g}^{-1}$  solution with 2%  $\text{HNO}_3$  using an electronic micropipette ( $50\text{--}1000 \text{ }\mu\text{L}$ , precision  $< 0.6\%$ , Eppendorf) just before instrumental analyses. Mercury loss was monitored every 10 minutes for one hour from solutions contained in four different types of containers: HDPE (15 mL centrifuge tube, BD Falcon), PTFE (15 mL Teflon vial with closure, Savillex), PFA (20 mL bottle, As One), and amber glass bottle with Teflon lined cap (40 mL EPA vial, I-Chem). Bromine chloride (BrCl) and gold chloride ( $\text{AuCl}_3$ ) were tested as preservatives against Hg loss. BrCl, an oxidizing agent generally used to determine  $\text{Hg}_T$  in cold vapor generation methods, was prepared following the U. S. Environmental Protection Agency (US EPA) method 245.7 "Mercury in water by cold vapor atomic fluorescence spectrometry"; it was added to  $20 \text{ pg g}^{-1}$  standard solution in HDPE tube to the final concentration of 0.5% (v/v) in 2%  $\text{HNO}_3$  matrix. US EPA also recommends stabilizing Hg using  $1 \text{ }\mu\text{g g}^{-1}$   $\text{AuCl}_3$  in 2%  $\text{HNO}_3$ .<sup>19</sup> However, we lowered the  $\text{AuCl}_3$  concentration to  $100 \text{ ng g}^{-1}$ , considering the Hg impurity in commercial  $\text{AuCl}_3$  solutions ( $1000 \text{ mg L}^{-1}$  ICP single element standard, Inorganic Ventures Inc.). The standard solution with  $100 \text{ ng g}^{-1}$   $\text{AuCl}_3$  in amber glass bottle was also monitored every 10 minutes for an hour and was found to be stable.

## Results and Discussion

**Mercury Loss from Dilute Standard Solutions.** The temporal evolution of Hg loss in different types of containers is shown in Figure 2(a). Both HDPE and Teflon (PFA and PTFE) incurred significant loss of  $0.09\text{--}0.15 \text{ pg Hg g}^{-1} \text{ min}^{-1}$ . Although Teflon was expected to be superior to HDPE against Hg loss,<sup>16</sup> both PFA and PTFE failed to preserve Hg for the monitoring duration of one hour (Fig. 2(a)). They showed slightly improved retention of  $50 \text{ pg g}^{-1}$  Hg in 1% (v/v)  $\text{HNO}_3$  only over longer term (5 hours): 82% (PTFE) versus 77% (LDPE) (not shown). The glass bottle retained Hg fairly well, with all results falling within 10% of the initial value (Fig. 2(a)). However, loss comparable to the HDPE was irregularly experienced (not shown), perhaps due to imperfect sealing of the vial. For this reason, we decided to further add preservatives to stabilize the Hg.

The strong oxidant BrCl has been used effectively for Hg fixation in solution, as for the ORMS-4 reference material kept in a glass ampule. For the HDPE bottle, adding BrCl to the same level as for the ORMS-4 (0.5% (v/v)) also appeared to be efficient against Hg loss (Fig. 2(b)). Alternatively, the addition of  $\text{AuCl}_3$  at a tenth ( $100 \text{ ng g}^{-1}$ ) of the US EPA recommended concentration retained  $\text{Hg}_T$  in the glass bottle (Fig. 2(b)). The irregular loss experienced with glass bottles was overcome with  $\text{AuCl}_3$  addition. Injection of

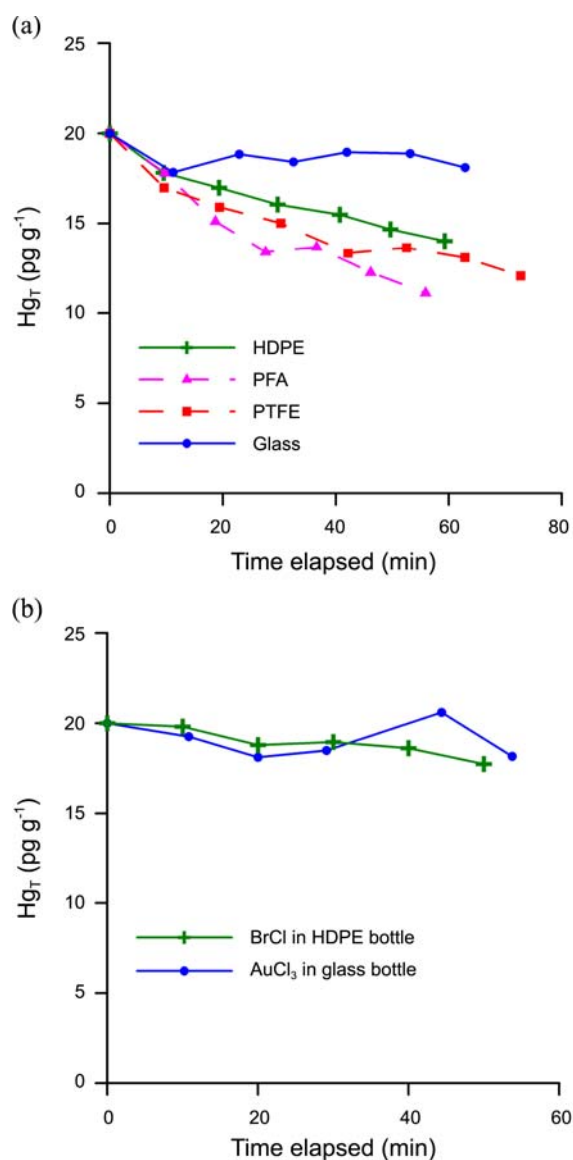


**Figure 2.** Mercury loss from  $20 \text{ pg g}^{-1}$  Hg standard solutions for (a) different container material and (b) different preservatives ( $0.5\%$  (v/v) BrCl and  $100 \text{ ng g}^{-1}$   $\text{AuCl}_3$ ).

BrCl or  $\text{AuCl}_3$  into the instrument can cause transient increase of the Hg signal, because they are more efficient than the wash solution (2%  $\text{HNO}_3$ ) in mobilizing Hg from the sample introduction system. Therefore, use of preservatives required additional time for washing and conditioning.

The loss of Hg from standards leads to its overestimation in the sample, and the discrepancy increases with time. Applying the determined loss rate ( $0.09\text{--}0.15 \text{ pg Hg g}^{-1} \text{ min}^{-1}$ ) of the  $20 \text{ pg g}^{-1}$  Hg standard solution, a delay of 10 minutes from the time of standard preparation would result in about 5–8% overestimation (Fig. S1). Factors such as bottle size, shape, and seal could change the loss rate.

In summary, immediate analyses of the working standards within a few minutes of dilution is a practical approach if an error range of 5–8% is acceptable. For better results, use of

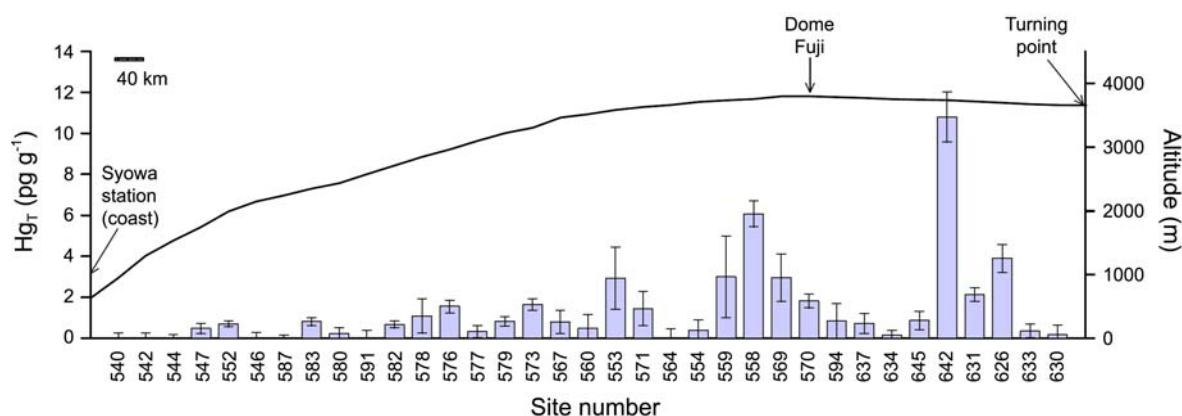


**Figure 3.** Total mercury concentrations of surface snow samples (SS1 series) collected along the traverse shown in Fig. 1. These are underestimates due to potential mercury loss from the snowmelt samples. The error bars indicate  $1\sigma$  instrumental precision.

glass containers with Teflon seals and addition of an appropriate preservative effectively prevents Hg loss. In this study, we used glass containers and  $\text{AuCl}_3$  for preparation of working standards.

**Hg<sub>T</sub> of Surface Snow Samples.** Total mercury in the surface snow samples (SS1,  $n = 35$ ) varied from below detection limit ( $0.4 \text{ pg g}^{-1}$ ) ( $n = 12$ ) to  $10.8 \pm 1.2 \text{ pg g}^{-1}$  ( $1\sigma$  instrumental precision) (Fig. 3; Table S2).

**Mercury Loss in Snow Samples.** The SS2 series samples ( $n = 9$ ) suffered Hg loss similar to the dilute working standards. Of the nine samples, seven with original  $\text{Hg}_T < 2 \text{ pg g}^{-1}$  fell below detection limit on the second analysis, and two with original  $\text{Hg}_T > 2 \text{ pg g}^{-1}$  (samples 574 and 628) lost 52% and 37%, respectively, of the original  $\text{Hg}_T$  (Fig. 5; Table S3). The loss of Hg from SS2 series samples implies that the SS1 series could also have experienced loss between aliquoting and analysis, making our  $\text{Hg}_T$  measurements underestimates. The ratio of  $\text{Hg}_T$  before and after storage is not unique for all SS2 samples and suggests that the actual amount in SS1 can be approximately 2-5 times higher than what we measured.

It appears that the labile species of mercury in snow becomes volatile during melting and in the liquid state. Loss during transportation and storage is probably minimal since the samples were kept frozen in the dark to prevent photochemical redox reaction. Hg evasion during snowmelt has been observed in field studies,<sup>20-22</sup> and laboratory experiments have also demonstrated increasing GEM flux as snow is melted.<sup>20</sup> However, there have also been cases where only partial or no loss occurred,<sup>15,17</sup> implying that the extent of Hg loss is dependent on factors such as Hg speciation and the chemical composition of the snowmelt matrix.

**Spatial Variation of Mercury from the Coast Inland.** High  $\text{Hg}_T$  values above the third quartile ( $> 1.7 \text{ pg g}^{-1}$ ) were observed only in the inner Plateau ( $> 570 \text{ km}$  from the sea ice,  $> 3500 \text{ m}$  altitude) (Figs. 3, 4; Table S2). The average  $\text{Hg}_T$  inland of site 560 is higher than that seaward of site 560 (Student's  $t$ -test, 95% confidence level). However, no significant trend was observed with distance from the sea ice ( $r^2 = 0.19$ ) or with altitude ( $r^2 = 0.15$ ) (Fig. 4). A consistent

spatial trend of  $\text{Hg}_T$  in surface snow was found only within a short distance ( $< 100 \text{ km}$ ):  $\text{Hg}_T$  gradually diminishing with distance inland from the edge of the sea ice, probably owing to the decreased supply of marine halogens for photo-oxidation of GEM.<sup>13,23</sup> For example, at McMurdo  $\text{Hg}_T$  decreased unevenly from 440 to  $70 \text{ pg g}^{-1}$  within approximately 30 km,<sup>13</sup> and Cornwallis Island in the Arctic from 17 to  $2 \text{ pg g}^{-1}$  within approximately 80 km.<sup>23</sup> Our samples were collected along a much longer distance, and various factors could be obscuring a spatial trend. First, although direct transport of sea-salt decreases with distance from the coast, there could also be recycling of deposited halogens.<sup>24,25</sup> Additionally, our most seaward sample (site 540) is already at an altitude of 948 m (Fig. 1, Tables 1, S2). Hence, none of our samples is truly coastal. Second, the period of 1.5 months taken for the traverse from the Syowa Station to the turning point could have allowed varying degrees of depositional and post-depositional photochemical processes at coastal versus inland sites. Third, a given thickness of surface snow layer at an inland site integrates over a longer time interval than an

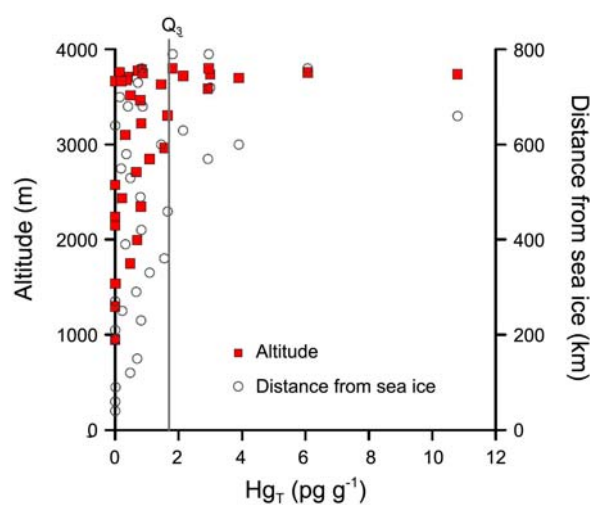


**Figure 4.** The relationship between total mercury and altitude (m) and distance from sea ice (km) for SS1 series.  $Q_3$  indicates the third quartile ( $1.7 \text{ pg g}^{-1}$ ).

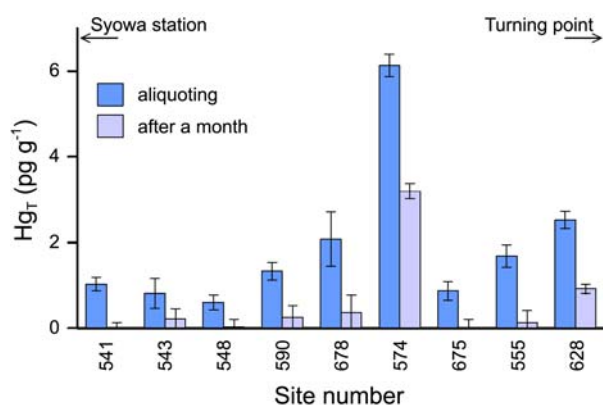


**Figure 5.** Duplicate analyses of the surface snow samples (SS2 series) analyzed a month apart. The error bars indicate 1 $\sigma$  instrumental precision.

equivalent thickness of surface snow layer near the coast because of the lower accumulation rate in the interior. Fourth, long-range transport and vertical precipitation of Hg from the stratosphere could be more pronounced on the inner Plateau.

The magnitude of spatial plus temporal variability can be gauged from the comparison of samples 590 vs. 678 and samples 574 vs. 675 in SS2 (Fig. 5). Each pair was obtained at the same sites albeit at different times (Fig. 1). The first pair coincided within uncertainty but the second pair exhibited a large discrepancy of a factor of 7 ( $\sim 5$  pg g<sup>-1</sup>) (Fig. 5).

**Low Hg<sub>T</sub> in Surface Snow: Low Photo-oxidation or High Photo-reduction?** Published Hg concentrations of Antarctic snow fall into two distinct categories: high (40 to hundreds of pg g<sup>-1</sup>) and low (< 40 pg g<sup>-1</sup>) (Table 1). Lack of precise information on the sampling strategies and use of diverse analytical techniques make direct comparison difficult. Some studies do not report the sampling dates and the effect of temporal variation in the magnitude of photochemical oxidation of Hg cannot be appraised. In terms of analytical methods, the cold vapor generation method measures soluble inorganic Hg that can be readily reduced to elemental mercury, whereas the ICP-MS technique measures total mercury, i.e. all that can be ionized in the hot plasma. Even allowing for the temporally variable Hg<sub>T</sub> level in surface snow and potential underestimation of SS1 series samples, it is still notable that our samples fall in the “low” category.

Total mercury in snow is balanced by deposition and re-emission fluxes in the course of photochemical redox processes.<sup>4</sup> The quasi-permanent sequestration of Hg by the polar snowpack then should be determined by how long the snowpack resides above the sunlight penetration depth and how fast the reactive Hg<sup>II</sup> in the snowpack is re-emitted as a consequence of photochemical reduction within the sunlit layer. The prevailing oxidation of atmospheric GEM to RGM after polar sunrise and subsequent deposition was postulated as cause for the high Hg<sub>T</sub> in surface snow at two dome sites.<sup>11,12</sup> It is proposed that three factors regulate the

atmospheric mercury oxidation and deposition – (1) supply of halogen radicals, (2) thickness of the turbulent mixing layer, and (3) amount of snowfall.

First, halogen radicals (e.g. Br $\cdot$ , BrO $\cdot$ , and Cl $\cdot$ ) play a key role in the oxidation of atmospheric GEM. Although they are concentrated near sea-ice regions,<sup>9</sup> long-range transport and recycling of sea-salt appear to supply marine halogens even to the inland Plateau.<sup>25</sup> Sea-salt particles on Dome Fuji preferentially liberate Cl $^-$  and Br $^-$  in austral summer,<sup>24</sup> allowing GEM oxidation to advance.<sup>11</sup> Thus, the interior location in itself should not hinder Hg deposition on surface snow.

Second, the atmospheric turbulent layer encourages entrainment of RGM from the free troposphere during the sunlit period,<sup>11</sup> populating RGM near surface snow and subsequently depositing them. The thickness of the turbulent layer at Dome Fuji remains at  $\sim 20$  m in winter but increases (up to  $\sim 300$  m with diurnal variation) in summer.<sup>26,27</sup> Therefore, the thickness of the turbulent layer should not limit surface Hg deposition at Dome Fuji.

Third, under the severely dry climatic condition of our sampling site, the low snowfall (< 10 cm yr<sup>-1</sup>)<sup>28</sup> could limit scavenging and deposition of RGM.<sup>29</sup> However, dry deposition of RGM to the snowpack provides an alternative pathway<sup>22</sup> and hence the low snowfall cannot be the cause of low Hg deposition at our site.

Thus, our samples satisfy the conditions of the “high Hg<sub>T</sub>” category (thick turbulent layer, recycling of halogens) yet exhibit low Hg<sub>T</sub>. The low Hg<sub>T</sub> levels must be due to an as-yet-unidentified factor for GEM oxidation or to active post-depositional reduction.

Post-depositional photo-reduction causes re-emission of Hg from the surface snow and contributes to the temporal heterogeneity of Hg<sub>T</sub> in snow.<sup>20,30</sup> Up to 40-54% of deposited Hg is released back to the atmosphere within 24 hours by photo-induced reduction in the temperate suburban areas<sup>10,31</sup> and up to 92% within 2 days after AMDE in the Arctic.<sup>32</sup>

The extremely low (sometimes negative) accumulation rate on the inner Plateau compared to the coastal region exposes the snowpack to sunlight for a longer period. At Dome Fuji, the annual accumulation rate is as low as 10 cm yr<sup>-1</sup> and is slightly lower during the austral summer than winter.<sup>28</sup> Assuming the effective penetration depth of sunlight to be greater than 10 cm,<sup>33,34</sup> the surface snow once deposited should reside within the sunlit layer for at least a year, allowing ample time for post-depositional photo-reduction. The lifetime of Hg<sup>II</sup> in the snowpack under solar irradiation is estimated to be 1-6 hours<sup>17</sup> but is subject to change depending on the chemical composition and physical property of the snow and ambient climatic conditions.<sup>4</sup> The poorly understood dynamics and factors influencing the post-depositional fate of Hg do not allow us to draw an unequivocal conclusion regarding the reason for the low Hg<sub>T</sub> in our surface snow samples. Future studies on mass-independent fractionation of mercury isotopes associated with photochemical reactions<sup>35</sup> and continuous monitoring

of atmospheric Hg species are expected to be helpful.

**Refractory Mercury.** The fraction of Hg in snow resistant to evasion during melting and to photo-reduction is destined for long-term sequestration.<sup>10,15,17</sup> We speculate that the major component of this refractory fraction is inorganic/organic particle-bound Hg, based on the sample behavior during ICP-SF-MS analyses and ice core records. The particle-bound fraction not oxidized by BrCl in conventional cold vapor generation method is decomposed at the high temperatures of the plasma.<sup>15</sup> The high Hg<sub>T</sub> of some samples analyzed by ICP-SF-MS was accompanied by large uncertainties (Fig. 3; Fig. 5 of reference 15; Fig. 1 of reference 36), which can be explained by inhomogeneous distribution of particles in the snowmelt and their efficient decomposition in the plasma. Such associations would not be observed in data obtained with conventional methods which only detect total soluble Hg.

The 670-kyr record of the Dome C ice core shows Hg<sub>T</sub> enhancements concurrent with increases of dust particle input during cold climate stages.<sup>36</sup> Particles scavenge RGM from the atmosphere, but the particle-bound Hg resists photo-reduction and is eventually sequestered in snow. Nearby volcanic eruptions or drier climate conditions can induce influx of particles to the Antarctic Plateau and promote Hg sequestration. Our hypothesis about the long-term sequestration of Hg by refractory particles can be tested by investigating vertical profiles of mercury in snow pits at high resolution to obtain seasonal to annual Hg<sub>T</sub> variations and episodic events like volcanic eruptions.

### Conclusions

We obtained new Hg<sub>T</sub> data of Antarctic surface snow that are near-contemporaneous (< 1.5 month) and spatially extensive (~1500 km traverse).

On the analytical side, we found that use of glass bottles and addition of 100 ng g<sup>-1</sup> AuCl<sub>3</sub> or 0.5% (v/v) BrCl prevent problematic Hg loss from dilute standard solutions. Some mercury loss also occurred in snowmelt samples, and we offer our Hg<sub>T</sub> measurements as lower limits.

The Hg<sub>T</sub> results displayed large spatial and/or temporal variation and were low compared to other Antarctic inland sites. This implies fast and/or spatially heterogeneous dynamics (oxidation-reduction) of Hg on the Antarctic snowpack. The factors that affect the long-term Hg sequestration are not fully understood, but snow accumulation rate and particle flux seem to be important.

**Supplementary Material.** Analytical details are available in the Supplementary Material (Fig. S1, Tables S1-S3).

**Acknowledgments.** This work was performed as part of the ITASE project, and we thank all field personnel in the 2007-2008 Japanese-Swedish IPY Antarctic expedition. This work was supported by the Mid-Career Researcher Program (No. 2010-0027586) through NRF grant funded by the MEST, KOPRI research grant (No. PE11090), and Inha

University research grant (No. INHA-42819-01).

### References

- Boutron, C. F. *Environ. Rev.* **1995**, *3*, 1.
- Schroeder, W. H.; Munthe, J. *Atmos. Environ.* **1998**, *32*, 809.
- Sheppard, D. S.; Patterson, J. E.; McAdam, M. K. *Atmos. Environ.* **1991**, *25*, 1657.
- Steffen, A.; Douglas, T.; Amyot, M.; Ariya, P.; Aspö, K.; Berg, T.; Bottenheim, J.; Brooks, S.; Cobbett, F.; Dastoor, A.; Dommergue, A.; Ebinghaus, R.; Ferrari, C.; Gardfeldt, K.; Goodsite, M. E.; Lean, D.; Poulain, A. J.; Scherz, C.; Skov, H.; Sommar, J.; Temme, C. *Atmos. Chem. Phys.* **2008**, *8*, 1445.
- Nguyen, H. T.; Kim, K.-H.; Shon, Z.-H.; Hong, S. *Crit. Rev. Environ. Sci. Technol.* **2009**, *39*, 552.
- Johnson, K. P.; Blum, J. D.; Keeler, G. J.; Douglas, T. A. *J. Geophys. Res.* **2008**, *113*, D17304.
- Lu, J.; Schroeder, W.; Barrie, L.; Steffen, A.; Welch, H.; Martin, K.; Lockhart, L.; Hunt, R.; Boila, G.; Richter, A. *Geophys. Res. Lett.* **2001**, *28*, 3219.
- Schroeder, W. H.; Anlauf, K. G.; Barrie, L. A.; Lu, J. Y.; Steffen, A.; Schneeberger, D. R.; Berg, T. *Nature* **1998**, *394*, 331.
- Ebinghaus, R.; Kock, H. H.; Temme, C.; Einax, J. W.; Löwe, A. G.; Richter, A.; Burrows, J. P.; Schroeder, W. H. *Environ. Sci. Technol.* **2002**, *36*, 1238.
- Lalonde, J. D.; Poulain, A. J.; Amyot, M. *Environ. Sci. Technol.* **2002**, *36*, 174.
- Brooks, S.; Arimoto, R.; Lindberg, S.; Southworth, G. *Atmos. Environ.* **2008**, *42*, 2877.
- Dommergue, A.; Sprovieri, F.; Pirrone, N.; Ebinghaus, R.; Brooks, S.; Courteau, J.; Ferrari, C. P. *Atmos. Chem. Phys.* **2010**, *10*, 3309.
- Brooks, S.; Lindberg, S.; Southworth, G.; Arimoto, R. *Atmos. Environ.* **2008**, *42*, 2885.
- Dick, A. L.; Sheppard, D. S.; Patterson, J. E. *Atmos. Environ.* **1990**, *24*, 973.
- Planchon, F. A. M.; Gabrielli, P.; Gauchard, P. A.; Dommergue, A.; Barbante, C.; Cairns, W. R. L.; Cozzi, G.; Nagorski, S. A.; Ferrari, C. P.; Boutron, C. F.; Capodaglio, G.; Cescon, P.; Varga, A.; Wolff, E. W. *J. Anal. At. Spectrom.* **2004**, *19*, 823.
- Parker, J. L.; Bloom, N. S. *Sci. Total Environ.* **2005**, *337*, 253.
- Dommergue, A.; Bahlmann, E.; Ebinghaus, R.; Ferrari, C.; Boutron, C. *Anal. Bioanal. Chem.* **2007**, *388*, 319.
- Hong, S.; Lluberas, A.; Rodriguez, F. *Korean J. Polar Res.* **2000**, *11*, 35.
- Butler, L. C.; Pearson, G. *Mercury Preservation Techniques*, US Environmental Protection Agency, 2003, <http://www.epa.gov/esd/tsc/fact-sheets.htm>.
- Faïn, X.; Grangeon, S.; Bahlmann, E.; Fritsche, J.; Obrist, D.; Dommergue, A.; Ferrari, C. P.; Cairns, W.; Ebinghaus, R.; Barbante, C.; Cescon, P.; Boutron, C. *J. Geophys. Res.* **2007**, *112*, D21311.
- Dommergue, A.; Ferrari, C. P.; Gauchard, P.-A.; Boutron, C. F.; Poissant, L.; Pilote, M.; Jitaru, P.; Adams, F. C. *Geophys. Res. Lett.* **2003**, *30*, 1621.
- Lindberg, S. E.; Brooks, S.; Lin, C. J.; Scott, K. J.; Landis, M. S.; Stevens, R. K.; Goodsite, M.; Richter, A. *Environ. Sci. Technol.* **2002**, *36*, 1245.
- Poulain, A. J.; Garcia, E.; Amyot, M.; Campbell, P. G. C.; Ariya, P. A. *Geochim. Cosmochim. Acta* **2007**, *71*, 3419.
- Hara, K.; Osada, K.; Kido, M.; Hayashi, M.; Matsunaga, K.; Iwasaka, Y.; Yamanouchi, T.; Hashida, G.; Fukatsu, T. *J. Geophys. Res.* **2004**, *109*, D20208.
- Suzuki, T.; Iizuka, Y.; Matsuoka, K.; Furukawa, T.; Kamiyama, K.; Watanabe, O. *Tellus B* **2002**, *54*, 407.
- Swain, M. R.; Gallée, H. *Pub. Astron. Soc. Pacific* **2006**, *118*, 1190.
- Takato, N.; Ichikawa, T.; Uruguchi, F.; Lundock, R.; Murata, C.; Taniguchi, Y.; Motoyama, H.; Fukui, K.; Taguchi, M. *Eur. Astron.*

- Soc. Pub. Series* **2008**, 33, 271.
28. Kameda, T.; Motoyama, H.; Fujita, S.; Takahashi, S. *J. Glaciol.* **2008**, 54, 107.
29. Ferrari, C. P.; Padova, C.; Fa, X.; Gauchard, P.-A.; Dommergue, A.; Aspino, K.; Berg, T.; Cairns, W.; Barbante, C.; Cescon, P.; Kaleschke, L.; Richter, A.; Wittrock, F.; Boutron, C. *Sci. Total Environ.* **2008**, 397, 167.
30. Ferrari, C. P.; Gauchard, P.-A.; Aspino, K.; Dommergue, A.; Magand, O.; Bahlmann, E.; Nagorski, S.; Temme, C.; Ebinghaus, R.; Steffen, A.; Banic, C.; Berg, T.; Planchon, F.; Barbante, C.; Cescon, P.; Boutron, C. F. *Atmos. Environ.* **2005**, 39, 7633.
31. Lalonde, J. D.; Amyot, M.; Doyon, M.-R.; Auclair, J.-C. *J. Geophys. Res.* **2003**, 108, 4200.
32. Poulain, A. J.; Lalonde, J. D.; Amyot, M.; Sheard, J. A.; Raofie, F.; Ariya, P. A. *Atmos. Environ.* **2004**, 38, 6763.
33. King, M. D.; Simpson, W. R. *J. Geophys. Res.* **2001**, 106, 12499.
34. Warren, S.; Brandt, R.; Grenfell, T. *Appl. Opt.* **2006**, 45, 5320.
35. Sherman, L. S.; Blum, J. D.; Johnson, K. P.; Keeler, G. J.; Barres, J. A.; Douglas, T. A. *Nat. Geosci.* **2010**, 3, 173.
36. Jitaru, P.; Gabrielli, P.; Marteel, A.; Plane, J. M. C.; Planchon, F. A. M.; Gauchard, P. A.; Ferrari, C. P.; Boutron, C. F.; Adams, F. C.; Hong, S.; Cescon, P.; Barbante, C. *Nat. Geosci.* **2009**, 2, 505.
37. Witherow, R. A.; Lyons, W. B. *Environ. Sci. Technol.* **2008**, 42, 4710.
38. Vandal, G. M.; Fitzgerald, W. F.; Boutron, C. F.; Candelone, J. P. In *Ice Core Studies of Global Biogeochemical Cycles*; Delmas, R. J., Ed.; Springer-Verlag: Berlin, Germany, 1995; p 401.
-